Chemical Mechanism of DNA Cleavage by the Homing Endonuclease I-*Ppo*I†

Stephen J. Mannino,‡ Cara L. Jenkins,§ and Ronald T. Raines*,‡,§

Department of Biochemistry and Department of Chemistry, University of Wisconsin—Madison, Madison, Wisconsin 53706

Received June 24, 1999; Revised Manuscript Received September 1, 1999

ABSTRACT: Homing endonucleases are distinguished by their ability to catalyze the cleavage of double-stranded DNA with extremely high specificity. I-*Ppo*I endonuclease, a homing endonuclease from the slime mold *Physarum polycephalum*, is a small enzyme (2 × 20 kDa) of known three-dimensional structure that catalyzes the cleavage of a long target DNA sequence (15 base pairs). Here, a detailed chemical mechanism for catalysis of DNA cleavage by I-*Ppo*I endonuclease is proposed and tested by creating six variants in which active-site residues are replaced with alanine. The side chains of three residues (Arg61, His98, and Asn119) are found to be important for efficient catalysis of DNA cleavage. This finding is consistent with the proposed mechanism in which His98 abstracts a proton from an attacking water molecule bound by an adjacent phosphoryl oxygen, Arg61 and Asn119 stabilize the pentavalent transition state, and Asn119 also binds to the essential divalent metal cation (e.g., Mg^{2+} ion), which interacts with the 3′-oxygen leaving group. Because Mg^{2+} is required for cleavage of a substrate with a good leaving group (*p*-nitrophenolate), Mg^{2+} likely stabilizes the pentavalent transition state. The pH-dependence of k_{cat} for catalysis by I-*Ppo*I reveals a macroscopic pK_a of 8.4 for titratable groups that modulate product release. I-*Ppo*I appears to be unique among known restriction endonucleases and homing endonucleases in its use of a histidine residue to activate the attacking water molecule for in-line displacement of the 3′-leaving group.

Homing endonucleases, like type II bacterial restriction endonucleases, catalyze the hydrolytic cleavage of DNA in a site-specific manner, resulting in free 5′-phosphoryl and 3′-hydroxyl groups. Yet, the recognition sequences of homing endonucleases are, in general, substantially longer than are those of restriction endonucleases. Recognition sequences of homing endonucleases range from 15 to 40 base pairs (*1*, *2*), and these enzymes show degeneracy in the recognition of these target sites that resembles the degeneracy of transcription factors (*3*, *4*). In vivo, homing endonucleases function to initiate the process of intron homing, a gene conversion event involving the site-specific transfer of a mobile group I intron from an intron-containing allele to an intron-lacking one (*5*). The homing endonuclease initiates this process by generating a double-stranded break in the recipient sequence.

In 1989, Vogt and co-workers reported that a mobile group I intron in the nuclear extrachromosomal rDNA[1] of the Carolina strain of the slime mold *Physarum polycephalum* encoded a site-specific endonuclease capable of cleaving recipient rDNA at the site of intron integration (*6*). This endonuclease, I-*Ppo*I [for nomenclature, see ref *7*], recognizes a large, somewhat asymmetric sequence of DNA. The endonuclease binds to its target sequence CTCTCTTAA|GGTAGC (*8*) in the absence of Mg^{2+}, but requires a divalent metal cation as its only cofactor for cleavage (*9*). Catalysis of DNA cleavage results in product fragments with a 4-nt overhang on the 3′ ends (*8*, *10*). The enzyme is optimally active at basic pH (pH 10) (*11*), but is only slightly less active at more neutral pH (pH 7.5) (*9*). Alternative translation start sites, one near the beginning of the intron and the other in the upstream exon (*12*), result in proteins of 163 and 185 amino acid residues, respectively (*10*). Both forms are active enzymes, and it is not known which predominates in vivo.[2]

Recently, Stoddard, Monnat, and their co-workers reported the three-dimensional structures of crystalline I-*Ppo*I complexed with either 3′-thio-substituted substrate DNA or product DNA following cleavage (*13*, *14*). Residues in the active-site region include Arg61, His78, His98, His101, Thr103, and Asn119. There is only one unambiguously identified Mg^{2+} ion in each active site. This cation appears to be coordinated octahedrally by the side-chain oxygen of Asn119, the scissile phosphoryl group, and water molecules. In the product complex, the leaving group oxyanion is observed to interact with the Mg^{2+} ion.

In this study, we examine these three-dimensional structures of the enzyme bound to DNA and propose a chemical

† S. J. M. was supported by Molecular Biophysics Training Grant GM08293 (NIH). C. L. J. was supported by Chemistry-Biology Interface Training Grant GM08506 (NIH).

* To whom correspondence should be addressed. Telephone: (608) 262-8588. Fax: (608) 262-3453. E-mail: raines@biochem.wisc.edu.

‡ Department of Biochemistry.

§ Department of Chemistry.

[1] Abbreviations: BSA, bovine serum albumin; CAPS, 3-[cyclohexylamino]-1-propanesulfonic acid; CHES, 2-[*N*-cyclohexylamino]-ethanesulfonic acid; dsDNA, double-stranded DNA; DTT, dithiothreitol; IPTG, isopropyl-1-thio-β−D-galactopyranoside; MES, 2-[*N*-morpholino]-ethanesulfonic acid; MOPS, 3-[*N*-morpholino]-propanesulfonic acid; nt, nucleotide; PDB, Protein Data Bank; rDNA, ribosomal DNA.

[2] The amino acid numbering system used herein is that of the smaller (163-residue) form of I-*Ppo*I because this form was used in the determination of the three-dimensional structure. The studies presented here utilize the longer form of the enzyme, which forms a homodimer of 20-kDa subunits in solution (*8*).

10.1021/bi991452v CCC: $18.00
Published on Web 11/17/1999

mechanism for catalysis of DNA cleavage. We then test this mechanism by replacing six active-site residues individually with alanine and assessing the ability of the variant enzymes to catalyze DNA cleavage. We find three residues that are critical to catalysis: Arg61, His98, and Asn119. Studies with an activated substrate, which does not require stabilization of its leaving group, enable us to reveal multiple roles for the Mg^{2+} ion. Finally, we examine the pH-dependence of k_{cat} and find that the rate of product release, which appears to be rate-limiting, is dependent on the titration of one or more groups with a macroscopic pK_a value of approximately 8.4.

EXPERIMENTAL PROCEDURES

Materials. All chemicals were from Fisher Scientific (Pittsburgh, PA) unless noted otherwise. Enzymes used for DNA manipulation were from Promega (Madison, WI) or New England Biolabs (Beverly, MA). CAPS, CHES, MES, and MOPS buffers and Gdm-Cl were from Sigma Chemical (St. Louis, MO). IPTG was from Gold Biotechnologies (St. Louis, MO). Bacto tryptone and Bacto yeast extract were from Difco (Detroit, MI).

General Methods. *Escherichia coli* strain BL21(DE3) (F^- ompT rB^- mB^-) and the pET-22b(+) expression vector were from Novagen (Madison, WI). Terrific Broth (*15*) medium (1.0 L) contained Bacto tryptone (12 g), Bacto yeast extract (24 g), glycerol (4 mL), KH_2PO_4 (2.31 g), and K_2HPO_4 (12.54 g). This medium was prepared using distilled, deionized water and autoclaved. *E. coli* cell lysis was performed using a French pressure cell from SLM Aminco (Urbana, IL). UV absorbance measurements were made on a Cary Model 3 spectrophotometer (Varian, Palo Alto, CA).

DNA oligonucleotides for DNA sequencing and site-directed mutagenesis were from Integrated DNA Technologies (Coralville, IA). DNA for sequencing was prepared using the QIAprep Spin Miniprep Kit from Qiagen (Valencia, CA). Reagents for DNA sequencing were from Applied Biosystems (Foster City, CA). DNA was sequenced using an ABI 373 Automated DNA Sequencer (Applied Biosystems) at the University of Wisconsin Biotechnology Center.

Logic of Variant Design. An examination of the three-dimensional structures of crystalline I-*Ppo*I bound to DNA (*14*) revealed a water molecule that is poised for nucleophilic attack on the scissile phosphoryl group. On the basis of this assignment, the residues most likely to serve as a base to activate this attacking water molecule are two histidines: His78 and His98. To identify the base, each of these histidine residues was replaced with alanine. Asn119, on the other hand, appears to provide one coordinating ligand for the Mg^{2+} ion in the active site. Arg61 is observed to interact with the newly formed 5′-phosphate following catalysis; however, this residue may have an additional role in stabilizing a pentavalent transition state. We generated the N119A and R61A variants in order to reveal the roles of these residues in catalysis. The H101A and T103A variants were generated to examine, respectively, whether His101 plays a role in protonating the leaving group during catalysis and if Thr103 is involved in positioning the substrate for catalysis.

Production of I-PpoI Endonuclease in Escherichia coli. A cDNA encoding I-*Ppo*I was a generous gift of Volker M. Vogt. Primers for cDNA amplification were designed to yield *Nde*I and *Bam*HI restriction sites at the upstream and downstream ends, respectively, of the PCR product. The amplified I-*Ppo*I cDNA was digested with *Nde*I and *Bam*HI restriction endonucleases (Promega) and ligated to the same sites of a similarly digested and gel-purified pET-22b(+) expression vector (Novagen), yielding plasmid pET-IPPO. In pET-IPPO, expression of the I-*Ppo*I cDNA is under the control of the T7 promoter and the lac operator. Oligonucleotide-mediated site-directed mutagenesis (*16*) of pET-IPPO was used to replace Arg61, His78, His98, His101, Thr103, and Asn119 of I-*Ppo*I with alanine residues. Plasmid pET-IPPO (or the plasmid expressing one of the variants) was used to transform the expression host BL21(DE3) (Novagen).

To produce I-*Ppo*I, cultures (0.5 L) of transformed cells were grown in Terrific Broth medium supplemented with ampicillin (0.1 mg/mL) at 37 °C with shaking (220 rpm). When the cell density reached an OD of 2.0 at 600 nm, expression was induced by the addition of IPTG (0.5 mM). The cultures were allowed to continue shaking at 37 °C for an additional 2 h; the cells were then harvested by centrifugation at 4500*g* for 15 min at 4 °C. Pelleted cells were resuspended in 50 mL of 20 mM Tris-HCl buffer (pH 7.4) containing EDTA (1 mM) and NaCl (0.2 M) and lysed by 2 passes through a French pressure cell. Insoluble matter was separated from the soluble fraction by centrifugation at 16 000*g* for 40 min at 4 °C, and the two fractions were analyzed for the presence of I-*Ppo*I endonuclease by reducing SDS-polyacrylamide gel electrophoresis (SDS-PAGE). Virtually all of the I-*Ppo*I produced was found to be in the insoluble fraction as inclusion bodies.

Folding and Purification of I-PpoI Endonuclease. Inclusion body pellets were washed to remove lipids and nucleic acids in a manner similar to that used by Burgess and coworkers (*17*) with a few modifications. Briefly, the pellets were resuspended in 40 mL of 50 mM Tris-HCl buffer (pH 7.9) containing sodium deoxycholate (2% w/v), EDTA (0.1 mM), and glycerol (5% v/v) by rapid pipetting. The resuspended pellets were allowed to stir at 4 °C for 1.5 h. The washed inclusion body pellets were then harvested by centrifugation at 16 000*g* for 30 min at 4 °C. The inclusion bodies were then denatured by stirring at room temperature for 3 h in 30 mL of 10 mM Tris-HCl buffer (pH 8.0) containing Gdm-Cl (6 M), EDTA (1 mM), and DTT (0.1 M). The denaturation mixture was then centrifuged at 16 000*g* for 30 min at 4 °C to remove nonsolublized material. Denatured I-*Ppo*I was folded by dropwise addition of aliquots of Folding Buffer, which was 50 mM sodium phosphate buffer (pH 7.0) containing L-arginine (0.5 M), $MgSO_4$ (10 mM), $ZnCl_2$ (2 mM), and glycerol (5% v/v), to the denatured protein at 10 °C with constant stirring. The aliquots were added in such a way as to achieve an incremental reduction in Gdm-Cl concentration, and the folding mixture was allowed to stand at 10 °C for 20 min without stirring between each addition. Initially, the buffer was added to give a Gdm-Cl concentration of 2 M. Subsequent additions resulted in the following Gdm-Cl concentrations: 1.75, 1.5, 1.25, 1.0, 0.75, and 0.5 M. The final folding mixture (which contained 0.5 M Gdm-Cl) was allowed to stand at 10 °C without stirring for 10 h. The folded protein solution (0.36 L) was then concentrated by ultrafiltration using a YM10 membrane (10 000 M_r cutoff; Amicon, Beverly, MA) to a volume of

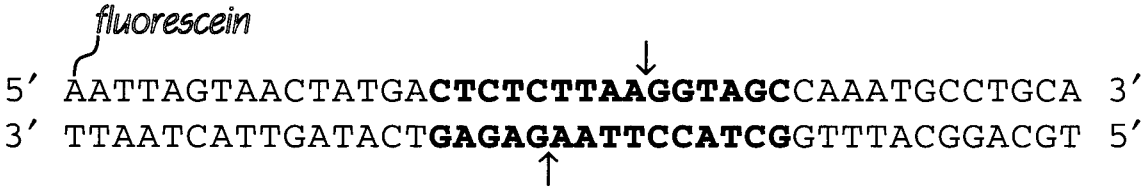

FIGURE 1: Sequence of the 42-bp DNA substrate used for assays to determine the effect of pH on values of k_{cat} for I-*Ppo*I endonuclease. A fluorescein tag is used to visualize the substrate and product after electrophoresis. The nucleotides in bold indicate the I-*Ppo*I recognition sequence; the arrows indicate the cleavage sites.

approximately 30 mL. This concentrate was then centrifuged at 16000*g* for 40 min at 4 °C to remove precipitated material and dialyzed against 4 L of 50 mM sodium acetate buffer (pH 5.0) containing EDTA (10 mM), NaCl (0.15 M), and glycerol (5% v/v). The dialysate was centrifuged (16000*g* for 40 min at 4 °C) to remove any precipitate, and this concentrated protein solution was filtered through a sterile 0.2-μm filter in preparation for purification by FPLC. At this stage, the protein was already approximately 90% pure as judged by SDS-PAGE.

Further purification was achieved by anion-exchange FPLC on a MonoS column from (Uppsala, Sweden). Protein was loaded in 50 mM sodium acetate buffer (pH 5.0) containing EDTA (10 mM) and NaCl (0.15 M) and eluted in a linear gradient of NaCl (0.15−0.58 M). I-*Ppo*I eluted in fractions corresponding to approximately 0.40 M NaCl. The fractions containing I-*Ppo*I were concentrated to an approximate volume of 1 mL using Centricon-10 centrifugal concentrators from Amicon. Protein was diluted with an equal volume of 50 mM sodium acetate buffer (pH 5.0) to reduce the salt concentration, passed through a 0.2 μm filter, aliquoted, frozen quickly, and stored at −70 °C. Concentrations of protein solutions were estimated by measuring the absorbance at 280 nm and using $\epsilon_{280} = 35\,000\ M^{-1}\ cm^{-1}$ (18).

Assay of Catalytic Activity. Relative activities of wild-type I-*Ppo*I and its variants were determined by incubating various amounts of enzyme with a substrate plasmid (p42) containing a single copy of the enzyme's recognition site, followed by comparison of intensity of bands corresponding to linear and supercoiled DNA in an agarose gel. Specifically, enzyme (0.10 ng − 2.5 μg) was incubated in a solution (20 μL) of either 25 mM CHES/25 mM CAPS buffer (pH 10.0) containing NaCl (50 mM), DTT (2 mM), $MgCl_2$ (10 mM), BSA (0.1 mg/mL), and p42 plasmid DNA (0.5 μg) (pH 10.0 conditions) or 10 mM Tris-HCl buffer (pH 7.5) containing NaCl (50 mM), DTT (2 mM), $MgCl_2$ (10 mM), BSA (0.1 mg/mL), and p42 DNA (0.5 μg) (pH 7.5 conditions). Incubations were carried out at 37 °C for 1 h. Reactions were quenched by the addition of gel-loading dye such that the final composition of the quenched solution was 1.7 mM Tris-HCl buffer (pH 7.5) containing EDTA (10 mM), bromophenol blue (0.04% w/v), xylene cyanol (0.04% w/v), and orange G (0.07% w/v) and incubation at 70 °C for 10 min. Electrophoresis in an agarose (0.8% w/v) gel followed by staining with ethidium bromide, visualization using a Fluorimager SI (Molecular Dynamics, Sunnyvale, CA), and quantitation of linear and supercoiled bands using ImageQuant software (Molecular Dynamics) allowed the estimation of cleavage activity. Comparison of cleavage activity of the variants to wild-type activity at each pH tested resulted in relative activities for the variants.

Circular Dichroism Spectroscopy. Circular dichroism (CD) spectroscopy was used to assess the secondary structure of variants of I-*Ppo*I with reduced activity. CD spectra were obtained using a quartz cuvette with a path length of 0.1 cm and an Aviv Model 62A Circular Dichroism Spectrometer from Aviv Associates (Lakeland, NJ). Protein was diluted to a final concentration of 50 μg/mL in 10 mM sodium phosphate buffer (pH 7.4) containing EDTA (0.1 mM) and NaCl (25 mM). Spectra were recorded from 193 to 260 nm at 25 °C, corrected for buffer, and converted to molar ellipticity. Spectra were also normalized to the spectrum of the wild-type enzyme at 204 nm. Additionally, the CD spectra of wild-type I-*Ppo*I and the R61A variant were recorded at 37 °C and pH 10.0. Specifically, protein was diluted to a final concentration of 50 μg/mL in 5 mM CHES/5 mM CAPS buffer (pH 10.0) containing EDTA (0.1 mM) and NaCl (25 mM). Spectra were collected from 193 to 260 nm at 37 °C, corrected for buffer, and converted to molar ellipticity.

Structural Analyses. Crystal structures were visualized using Protein Data Bank (PDB) entries 1A74 (I-*Ppo*I•thio-substituted DNA complex), 1A73 (I-*Ppo*I•product DNA complex), 1BHM (*Bam*HI•DNA complex), and 1SMN (*Serratia* nuclease) with the program MIDASPLUS (*19*). Overlay of I-*Ppo*I•thio-substituted DNA and *Bam*HI•DNA structures and the I-*Ppo*I and *Serratia* nuclease active sites was done by least-squares superposition using the Match function in MIDASPLUS.

Effect of pH on k_{cat}. Values of k_{cat} at various pHs were determined by incubating wild-type I-*Ppo*I with substrate, removing aliquots at various time points, quenching these aliquots, and analyzing them by electrophoresis in a gel composed of 45 mM Tris-boric acid buffer (pH 8.4) containing EDTA (0.1 mM), urea (8 M), and acrylamide: bis-acrylamide (19:1; 15% w/v). Quantitation of cleavage was achieved by scanning the gel using a Vistra FluorImager SI ImageQuant software from Molecular Dynamics (Sunnyvale, CA). The substrate for the reactions was a 42-bp duplex containing the I-*Ppo*I recognition sequence and labeled on one 5′ end with fluorescein (Figure 1). This substrate was synthesized as described previously (*9*). The fluorescein label allowed for facile detection and quantitation of cleaved product and uncleaved substrate. Specifically, enzyme (1−10 nM) was incubated at 37 °C in a solution (70 μL) of 40 mM buffer containing NaCl (0.10 M) and $MgCl_2$ (10 mM). The buffers were as follows: pH 3.0, citric acid; pH 4.0 and 5.0, succinic acid; pH 6.0, MES; pH 7.0, MOPS; pH 7.5, 8.0, and 8.5, Tris; pH 9.0 and 9.5, CHES; pH 10.0 and 11.0, CAPS; and pH 12.0, sodium phosphate. The concentration of the dsDNA substrate was always at least 10-fold higher than that of the enzyme. Aliquots (10 μL) were removed at time points from 0 to 80 min and quenched by

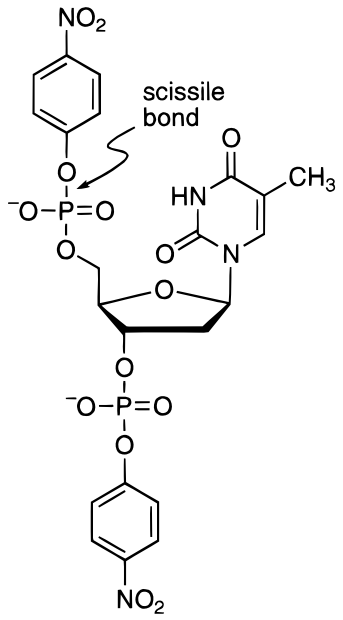

FIGURE 2: Structure of deoxythymidine 3′,5′bis-(*p*-nitrophenyl phosphate), an activated substrate for I-*Ppo*I endonuclease (*20*, *21*).

the addition of a formamide solution such that the resulting solution contained formamide (40% w/v), EDTA (10 mM), and bromophenol blue (0.25 mg/mL). Quantitation of cleavage following electrophoresis of these samples allowed for determination of V_{max} rather than V_{max}/K_m values from the linear initial velocity portion of plots of product concentration vs time. At all pHs tested, it was ensured that reaction conditions were such that V_{max} values were being obtained (substrate concentration $\gg K_M$). Division of these V_{max} values by the enzyme concentrations in the individual reactions yielded k_{cat} values. These k_{cat} values were then averaged and plotted vs pH.

Synthesis of Deoxythymidine 3′,5′-bis-(p-Nitrophenyl Phosphate). Cleavage of deoxythymidine 3′,5′-bis-(*p*-nitrophenyl phosphate) by I-*Ppo*I generates *p*-nitrophenolate (Figure 2) (*20*, *21*). Because *p*-nitrophenol has a pK_a of 7.14 (*22*), *p*-nitrophenolate is unlikely to need stabilization (e.g., by interaction with a Brønsted or Lewis acid) during catalysis of P−O bond cleavage. Accordingly, deoxythymidine 3′,5′-bis-(*p*-nitrophenyl phosphate) can serve as an effective probe for general acid catalysis by I-*Ppo*I (*23*, *24*).

Deoxythymidine 3′,5′-bis-(*p*-nitrophenyl phosphate) was synthesized as follows. Deoxythymidine (0.608 g, 2.51 mmol) and approximately 10 mL of pyridine freshly distilled over KOH were placed in an oven-dried flask. *p*-Nitrophenylphosphorodichloridate (1.305 g, 5.10 mmol) was added gradually by spatula, followed by additional pyridine (5 mL). The mixture was stirred at room temperature for 2 h, and then quenched by addition of ice-cold water (15 mL). This mixture was concentrated and placed under vacuum overnight. The resulting oil was suspended in water (50 mL) and extracted with chloroform (3 × 50 mL). The aqueous layer was concentrated (to 2 mL) under reduced pressure. This solution was adjusted to pH 4 with triethylamine. The product mixture was purified by anion-exchange chromatography on a column (25 cm × 20 cm^2) of DEAE Macro-Prep resin from Bio-Rad (Hercules, CA) that had been equilibrated with 0.1 M triethylammonium acetate buffer (pH 4). The loaded column was eluted with 0.1 M triethylammonium acetate buffer (pH 4), followed by 0.1 M triethylammonium acetate buffer (pH 8), and then by a linear gradient (0.25 L + 0.25 L) of triethylammonium bicarbonate buffer (pH 8; 0.1−1.2 M). The column was finally washed with 1.2 M triethylammonium bicarbonate buffer (pH 8). Fractions were monitored by UV spectroscopy in the wavelength range 250−500 nm, and those containing high absorbance at 275 nm and low absorbance at 312 nm (from *p*-nitrophenyl phosphate) and 400 nm (from *p*-nitrophenolate) were pooled and concentrated by lyophilization. The purified product was analyzed with a Bruker Reflex II MALDI-TOF mass spectrometry (calculated mass: 643.0; observed mass: 643.1). The concentration of solutions of deoxythymidine 3′,5′-bis-(*p*-nitrophenyl phosphate) was determined by measuring the absorbance at 275 nm and using $\epsilon_{275} = 22\,500$ M^{-1} cm^{-1} (*20*).

Catalysis of Deoxythymidine 3′,5′-bis-(p-Nitrophenyl Phosphate) Cleavage. Experiments assessing the cleavage of deoxythymidine 3′,5′-bis-(*p*-nitrophenyl phosphate) (Figure 2), an activated substrate for I-*Ppo*I, were carried out in a solution (0.12 mL) of 40 mM CHES buffer (pH 9.5) containing I-*Ppo*I (0.3 mg), deoxythymidine 3′,5′-bis-(*p*-nitrophenyl phosphate) (0.15 mM), and $MgCl_2$ (10 mM). The ability of both wild-type I-*Ppo*I and the N119A variant were assessed in this manner. Reactions of the wild-type enzyme in the absence of Mg^{2+} ion were performed with EDTA (10 mM) replacing the magnesium. Reactions were allowed to proceed for 20 min (in the presence of magnesium) or 4 h (in the absence of magnesium) at 25 °C, and product generation was monitored by UV-VIS spectroscopy at 400 nm. Reaction rates were determined by fitting the spectral data to a first-order exponential equation.

RESULTS

Gel-Based Activity Assays. The crystalline structures of I-*Ppo*I complexed with sulfur-substituted substrate DNA and product DNA are now known (*14*). From an examination of these structures, we targeted several residues in the active-site region for site-directed mutagenesis. We identified a water molecule that is poised for nucleophilic attack on the scissile phosphoryl group (Figure 3A−3C). This water molecule is coordinated by one of the nonbridging oxygen atoms of the adjacent 5′-phosphoryl group, a side-chain nitrogen of Arg61, and a side-chain nitrogen of either His78 or His98 (molecule A in Figure 3A−3C). We generated the H78A variant and the H98A variant to examine the importance of these residues to catalysis by I-*Ppo*I. We also substituted alanine for four other residues in the active-site region: Arg61, His101, Thr103, and Asn119. Asn119 coordinates the Mg^{2+} ion; and Arg61 could be involved in stabilizing a pentavalent transition state. The H101A and T103A variants were generated to examine whether either side chain participates in catalysis: His101 in protonating the leaving group and Thr103 in positioning the substrate DNA for catalysis. The catalytic activity of each variant was assessed by using the plasmid p42 substrate.

The T103A, H101A, and H78A variants all showed a level of activity near that of wild-type I-*Ppo*I. In contrast, the H98A and N119A variants both showed dramatically reduced catalytic activity against this plasmid substrate compared to

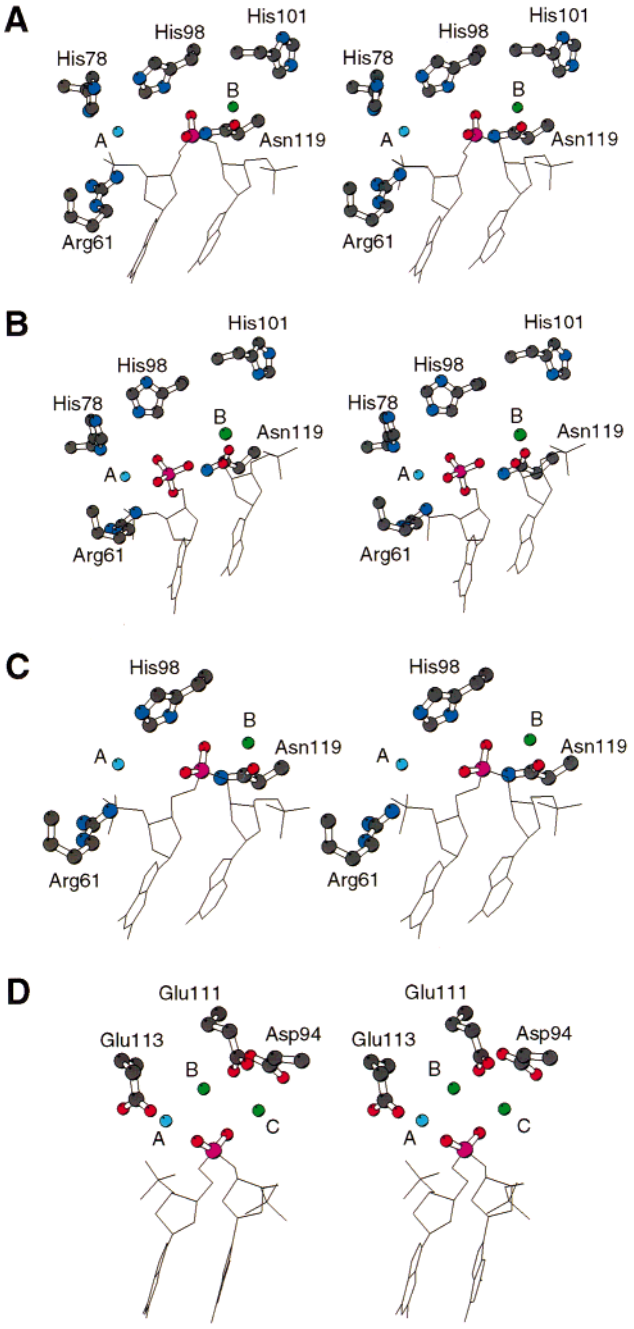

FIGURE 3: Stereoviews of the structures of the active-site regions of I-*Ppo*I endonuclease•DNA complexes (A−C) and a *Bam*HI endonuclease•DNA complex (D). The I-*Ppo*I structures are from PDB entries 1A74 (A and C) and 1A73 (B) (*14*); the *Bam*HI structure is from PDB entry 1BHM (32). In A−C, "A" represents our candidate for the attacking water molecule (HOH36 in PDB entry 1A74), and "B" is the site of the magnesium-water cluster. Thr103 was omitted for clarity. In D, "A" identifies the putative attacking water molecule, and "B" and "C" identify putative Mg^{2+} ion sites, with "B" activating the attacking water molecule. The relative orientation in C and D was generated by using the MATCH function in MIDASPLUS to align the DNA in the active sites of the two enzymes. This figure was created with the program MOLSCRIPT (*25*).

wild-type enzyme (Figure 4; Table 1). Attempts to rescue activity of the N119A variant by increasing the Mg^{2+} ion concentration were unsuccessful. Mg^{2+} ion concentrations up to 0.5 M failed to generate any detectable increase in the activity of the variant (data not shown).

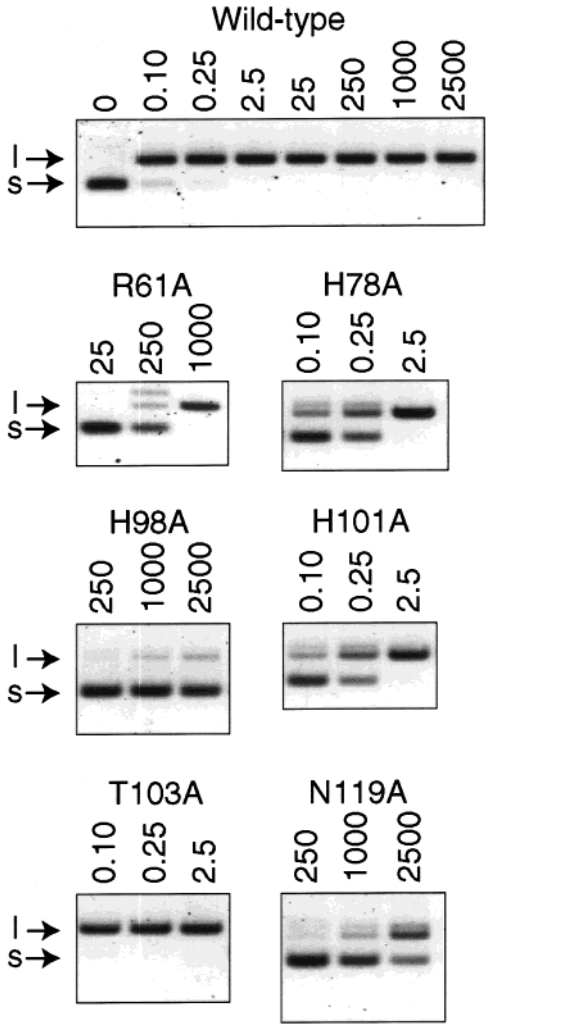

FIGURE 4: Agarose gels showing DNA cleavage by wild-type I-*Ppo*I endonuclease and its variants. Assay solutions (20 μL) contained enzyme (0.1 ng-2.5 μg) and p42 plasmid DNA (0.5 μg) in 25 mM CHES, 25 mM CAPS buffer (pH 10.0) containing NaCl (50 mM), $MgCl_2$ (10 mM), DTT (2 mM), and BSA (0.1 mg/mL). Reactions were allowed to proceed for 1 h at 37 °C before quenching and electrophoresis. The most informative enzyme concentrations are shown for each variant. Numbers above gel lanes represent amount of protein (ng) in the assay. Arrows labeled "l" and "s" indicate positions of the bands corresponding to linear and supercoiled plasmid DNA, respectively.

Results were similar at both pHs tested (pH 7.5 and pH 10.0) for all variants except for R61A I-*Ppo*I. This variant displays nearly wild-type activity at pH 7.5, but its activity is diminished drastically at pH 10.0 (Table 1). Thus, the catalytic activities of the variants described herein demonstrate the importance of three residues in the catalytic mechanism of I-*Ppo*I: Arg61, His98, and Asn119.

Circular Dichroism Spectra. The diminished catalytic activity of the H98A, N119A, and R61A variants could be due to an altered protein conformation rather than the absence of a functional group that participates in catalysis. To check for this possibility, we used CD spectroscopy, which is extremely sensitive to a protein's secondary structure (*26*). Spectra were collected from 193 to 260 nm at 25 °C and pH 7.4 for wild-type I-*Ppo*I and the H78A, H98A, and N119A variants. The spectra of all four proteins are essentially identical (data not shown). Spectra were also collected for wild-type I-*Ppo*I and the R61A variant at 37

Table 1: Relative Catalytic Activities of Wild-Type I-*Ppo*I Endonuclease and Variants[a]

enzyme	pH 7.5[b]	pH 10.0[c]
wild-type	1.0	1.0
R61A	0.47	0.000097
H78A	0.48	0.27
H98A	0.000026	0.0000065
H101A	1.3	0.26
T103A	0.96	1.1
N119A	0.000065	0.000078

[a] Relative activities at each pH were determined by extent of cleavage of p42 plasmid substrate DNA (0.5 μg) by various amounts of enzyme (0.1 ng−2.5 μg). Cleavage was estimated by quantitation of the linear and supercoiled bands after electrophoresis on an agarose gel. Values are the averages of at least three assays. [b] Assays were performed in 10 mM Tris-HCl buffer (pH 7.5) containing NaCl (0.10 M), $MgCl_2$ (10 mM), DTT (2 mM), and BSA (0.1 mg/mL). [c] Assays were performed in 25 mM CHES/25 mM CAPS buffer (pH 10.0) containing NaCl (50 mM), $MgCl_2$ (10 mM), DTT (2 mM), and BSA (0.1 mg/mL).

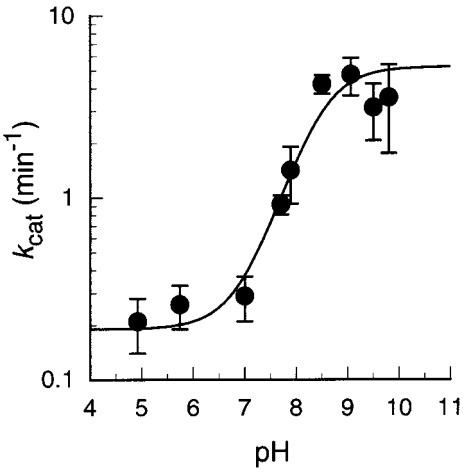

FIGURE 5: Plot showing the effect of pH of the value of k_{cat} for catalysis on DNA cleavage by I-*Ppo*I. The substrate for the reactions was a 42-bp DNA duplex (Figure 1). I-*Ppo*I (1−10 nM) was incubated in a solution (70 μL) of 40 mM buffer containing NaCl (0.10 M) and $MgCl_2$ (10 mM) at 37 °C. At all pH's tested, the substrate concentration was $\gg K_M$.

°C and pH 10.0 to examine the possibility that a pH-dependent conformational instability might be responsible for the loss of activity of this variant at pH 10.0. The spectra of the two proteins under this condition were also identical (data not shown). Apparently, the lower activities reported in Table 1 are due to the absence of side chains that participate in catalysis.

Effect of pH on k_{cat}. I-*Ppo*I was incubated with a fluorescein-labeled 42-bp substrate (Figure 1) at various pH values. Values of k_{cat} were calculated from the linear portion of a plot of product concentration vs time. The k_{cat} values were maximal at pH values of 9 and above. The k_{cat} vs pH data were fitted to an equation of the form: $k_{cat} = k_a/(1 + 10^{pH-pK_a}) + k_b/(1 + 10^{pK_a-pH})$ where k_a and k_b are rate constants when titratable groups are protonated (low pH) and deprotonated (high pH), respectively. The data fitted well to this model, with $k_a = 0.19$ min^{-1}, $k_b = 5.2$ min^{-1}, and $pK_a = 8.4$ (Figure 5). The sigmoidal shape of the pH − log k_{cat} profile (Figure 5), the similarity of the k_a and k_b values, and the high affinity of I-*Ppo*I for its cognate DNA (*9*) led us to conclude that pH-dependent product release rather than the chemical transition state limits catalysis.

Catalysis of Deoxythymidine 3′,5′-bis-(p-Nitrophenyl Phosphate) Cleavage. To examine whether the essential Mg^{2+} ion in the I-*Ppo*I active site performs functions in addition to stabilizing the 3′ oxyanion leaving group during catalysis of DNA cleavage, wild-type I-*Ppo*I was incubated with deoxythymidine 3′,5′-bis-(*p*-nitrophenyl phosphate), an activated substrate, in the presence and absence of Mg^{2+} ion. This substrate contains a good leaving group (*p*-nitrophenolate) and, unlike the 3′ oxyanion leaving group in DNA, should not require stabilization for cleavage to occur. The N119A variant was incubated with the substrate in the presence of Mg^{2+}. The reaction course was followed by monitoring the absorbance at 400 nm. Wild-type I-*Ppo*I was able to cleave deoxythymidine 3′,5′-bis-(*p*-nitrophenyl phosphate) (0.15 mM) in the presence of Mg^{2+} ion with a rate constant of approximately 0.29 min^{-1} at a substrate concentration of 0.15 mM. This value is similar to that reported previously (*31*). In contrast, there was no detectable cleavage of this substrate by I-*Ppo*I in the absence of Mg^{2+} ion or by the N119A variant in the presence of the divalent cation. On the basis of the detection limits of our assay, these rate constants must be <0.0001 min^{-1}.

DISCUSSION

Chemical Mechanism of I-PpoI Endonuclease. The crystalline structures of two I-*Ppo*I endonuclease•DNA complexes are now known (Figure 3A−3C)(*13*, *14*). In one complex, I-*Ppo*I is associated with a thio-substituted DNA ligand. In the other, the enzyme is complexed with product DNA after cleavage of a natural substrate. Both of these complexes contain a divalent metal cation in each active site. The metal cation in the product complex displays octahedral coordination by oxygens of the scissile phosphoryl group, the side-chain oxygen of Asn119, and water molecules. The thio-substituted structure is likely to approximate the substrate complex, which is stable because replacing the 3′-oxygen of the leaving group with sulfur inhibits cleavage. In the substrate complex, the thiol substitution for the 3′-oxygen of the DNA substrate appears to distort the metal coordination somewhat. There appear to be only four ligands to the metal ion, and the geometry is no longer octahedral. In this substrate complex, His98 is only 2.8 Å from the scissile phosphoryl group.

On the basis of these two structures, the crystallographers put forth a chemical mechanism for catalysis by I-*Ppo*I endonuclease. They proposed that, following cleavage, the scissile phosphoryl group moves toward Arg61, and His98 rotates to maintain contact with this phosphoryl group (Figure 3B). In addition, the 3′-oxygen of the leaving group becomes associated with the metal ion. Divalent metal cations are known to stabilize an oxyanion leaving group (*27*), and such stabilization has been postulated to occur during catalysis by Klenow exonuclease (*28*) and the *Tetrahymena* ribozyme (*29*). Finally, the crystallographers suggested that a metal-bound water molecule is the nucleophile (*14*). We disagree.

We put forth His98 as the base that activates the attacking water molecule. The greatly diminished catalytic activity of H98A I-*Ppo*I is consistent with this assignment (Table 1). The hydrolysis of phosphodiesters generally proceeds via in-line displacement of the 3′ leaving group by an activated water molecule (*30*) in a concerted S_N2 reaction (*31*).

Involvement of a metal-bound water as the attacking nucleophile as proposed (*14*) is difficult to reconcile with these geometric constraints (Figure 3A and 3C). The metal ion is interacting with the 3′-oxygen of the leaving group, and all water ligands of the metal ion have $H_2O-P-O^{3'}$ attack angles of less than 90°. In contrast, there is a water molecule that is positioned nearly linearly for in-line displacement of the 3′ leaving group (Figure 3A and 3C). This water molecule appears to form hydrogen bonds with the nonbridging oxygen of the 5′ adjacent phosphoryl group, $N_{\epsilon 2}$ of His98, and $N_{\eta 1}$ of Arg61 (vide infra).

Like His98, Asn119 could not be replaced without having a catastrophic effect on catalysis (Table 1). From the crystalline structure of I-*Ppo*I (*14*), it is clear that Asn119 provides both a coordinating ligand for the Mg^{2+} ion and a hydrogen bond donor to the scissile phosphoryl group. Loss of the metal ion would thus be expected to debilitate severely the enzyme's catalytic ability. It is not surprising that we were unable to rescue the activity of the N119A variant with high Mg^{2+} ion concentrations because the asparagine side chain is the only ligand provided by the protein.

R61A I-*Ppo*I suffers only a slight reduction in activity at pH 7.5. Thus, we conclude that Arg61 is not essential for binding the nucleophilic water molecule. The near wild-type activity of the R61A variant at pH 7.5 could be the result of another residue's performing the role normally played by Arg61. His78 is a strong candidate for such a residue because it is approximately equidistant from the scissile phosphoryl group. The pK_a of this histidine residue is likely to be higher in the R61A variant than in the wild-type enzyme because of the loss of unfavorable Coulombic interactions. Hence at the lower pH, His78 would be capable of substituting for Arg61 in donating a hydrogen bond, but at the higher pH it would not.

Cleavage of deoxythymidine 3′,5′-bis-(*p*-nitrophenyl phosphate) by I-*Ppo*I relies on Mg^{2+} ion as well as Asn119. We, therefore, conclude that the role of the essential Mg^{2+} ion is not limited to the stabilization of the 3′ leaving group. If this were its only role, then the cleavage of the activated substrate would likely be independent of Mg^{2+} ion. We propose that during catalysis, the Mg^{2+} ion interacts not only with the 3′ oxygen of the scissile phosphoryl group but also with a nonbridging oxygen of this same phosphoryl group. In this latter interaction, the Mg^{2+} ion acts as a Lewis acid to stabilize the accumulation of negative charge in the chemical transition state. The lack of activity of the N119A variant with deoxythymidine 3′,5′-bis-(*p*-nitrophenyl phosphate) is consistent with Asn119 playing the same role in the cleavage of both this substrate and DNA.

I-*Ppo*I is known to bind tightly to its substrate. The complex with the 42-bp duplex shown in Figure 1 has K_d = 3.4 nM in the presence of 0.10 M NaCl and the absence of Mg^{2+} ion (*9*). We find evidence that I-*Ppo*I also binds tightly to its product(s). The k_{cat} vs pH data for cleavage of a 42-bp substrate by I-*Ppo*I (Figure 5) is consistent with the release of product limiting the rate of DNA cleavage. The pK_a value obtained by fitting the data is approximately 8.4. This pK_a value is almost certainly a macroscopic pK_a that is actually composed of several microscopic pK_a values that cannot be resolved individually with our assay. Still, the observed pK_a of 8.4 is consistent with the involvement of one or more histidine residues in modulating the rate of product release. There are two histidine residues in the active site that are within hydrogen bonding distance of the bound DNA: His78 and His98. That the titration of His98 appears to affect the rate of product release is not at odds with its role as the base in the chemical mechanism of DNA cleavage by I-*Ppo*I. At high pH, the rapid deprotonation of this residue after the chemical transition state could facilitate product release.

Comparisons with Other Nucleases. In reporting the crystalline structure of the type II restriction endonuclease *Bam*HI complexed with DNA, Aggarwal and co-workers proposed a two-metal mechanism for cleavage (*32*). They identified the putative attacking water molecule and the two Mg^{2+}-ion binding sites and suggested that one of the metal ions is involved in deprotonating the attacking water. Interestingly, when we performed a least squares superposition of the DNA in the active-site regions of *Bam*HI and I-*Ppo*I structures, some similarities became evident (Figure 3C and 3D). First, the water molecule that Aggarwal and co-workers identify as the nucleophile is in a position similar to that of the water we have identified as the nucleophile in I-*Ppo*I. Both water molecules are positioned nearly linearly with respect to the scissile $P-O^{3'}$ bond, with an $H_2O-P-O^{5'}$ angle of 150° for *Bam*HI and 156° for I-*Ppo*I. Further, the two waters are approximately equidistant from the electrophilic phosphorus (4.4 Å for *Bam*HI and 3.0 Å for I-*Ppo*I). Aggarwal and co-workers identify two probable binding sites for Mg^{2+} ion in *Bam*HI. They assign one Mg^{2+} ion site as being involved, along with the side chain of Glu113, in deprotonating the attacking water. His98 occupies this region in the I-*Ppo*I active site. We believe that this histidine residue in I-*Ppo*I acts alone to deprotonate the attacking water molecule.

Another interesting similarity appears when comparing the active sites of I-*Ppo*I endonuclease and the *Serratia* nuclease. Structural analyses (*33*, *34*), site-directed mutagenesis studies (*35*), and experiments utilizing deoxythymidine 3′,5′-bis-(*p*-nitrophenyl phosphate) (*24*) with the *Serratia* nuclease have resulted in the identification of His89 as the base that activates the attacking water molecule, Asn119 as a coordinating ligand for the necessary Mg^{2+} ion, Arg57 as stabilizing the transition state, and Glu127 as coordinating the magnesium-water cluster. A least-squares superposition of His98 from the I-*Ppo*I active site (from the structure of the thio-substituted complex) and His89 from the *Serratia* nuclease (apoenzyme) active site reveals that the positions of the active-site residues Arg61 and Asn119 in I-*Ppo*I are similar to those of *Serratia* nuclease residues Arg57 and Asn119 (*21*, *36*). This structural similarity and that of the magnesium−water cluster (*34*) are consistent with similar roles for the active-site residues.[3] These comparisons, together with the activity data presented herein, are consistent with a mechanism that proceeds via the transition state shown in Figure 6. A similar mechanism has been inferred by Pingoud, Krause, and co-workers (*21*).

The mechanism of I-*Ppo*I is unique among enzymes that catalyze the site-specific cleavage of dsDNA in that it relies on a histidine residue to activate the attacking water molecule. The active sites of most restriction endonucleases studied thus far are composed of two acidic residues that

[3] There is no residue in I-*Ppo*I in a position similar to that of Glu127 of *Serratia* nuclease.

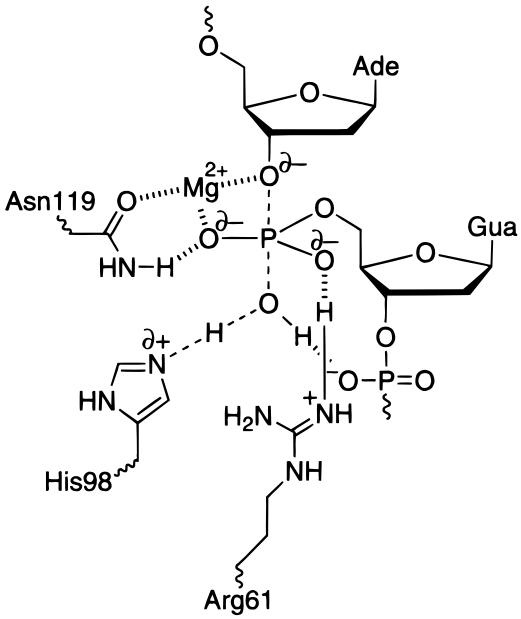

FIGURE 6: Putative structure of the transition state for catalysis of DNA cleavage by I-*Ppo*I endonuclease. The three residues shown are those identified herein to be essential for efficient catalysis.

are involved in coordinating metal ions or activating the attacking water molecule (or both) and a basic residue (usually lysine) that is involved in transition-state stabilization (*37*). The homing endonuclease PI-*Sce*I contains the same pattern of three catalytic residues in its active site (*38*). Both I-*Cre*I and I-*Ceu*I appear to require a glutamine residue for catalysis instead of one of the two acidic residues, and I-*Cre*I has an arginine residue in its active site instead of the lysine required by restriction endonucleases (*39*, *40*). Whereas I-*Ppo*I may be similar in that it requires an arginine and an asparagine residue, it is thus far unique in its absolute requirement for a histidine residue in order to catalyze dsDNA cleavage. Further, the attacking water molecule in most restriction endonucleases is believed to be activated either by a second metal ion in the active site or via substrate-assisted catalysis (*41*, *42*). In contrast, I-*Ppo*I appears to use the essential histidine residue as a base to activate the attacking water molecule. I-*Ppo*I is one of the first homing endonucleases to have its chemical mechanism examined by systematic site-directed mutagenesis of active-site residues. It will be interesting to see if other homing endonucleases also utilize a histidine residue as a base to activate the attacking water molecule.

Conclusion. Arg61, His98, and Asn119 are critically important residues in catalysis of DNA cleavage by I-*Ppo*I, as indicated by the diminished catalytic activity of the H98A and N119A variants at pH 7.5 and 10.0 and the R61A variant at pH 10.0. These data, along with an examination of the crystalline structure and comparisons with other structures, enabled us to propose a structure for the transition state of DNA cleavage (Figure 6). In our mechanism, His98 activates a water molecule for in-line attack on the scissile P−O bond. The side-chain nitrogens of Arg61 and Asn119 donate hydrogen bonds to nonbridging oxygens of the scissile phosphoryl group. The side-chain oxygen of Asn119 provides a ligand for the Mg^{2+} ion, which stabilizes the oxyanion leaving group. Because Mg^{2+} ion is required for cleavage of the activated substrate deoxythymidine-bis-3′,5′-(*p*-nitrophenyl phosphate), we propose that the Mg^{2+} ion also interacts with a nonbridging oxygen of the scissile phosphoryl group. His78, His101, and Thr103, though in the active site, do not appear to play critical roles in catalysis by I-*Ppo*I. The macroscopic pK_a of the titratable groups governing the rate of product release is approximately 8.4. Such a pK_a value is suggestive of the involvement of one or more histidine residues, such as His78 and His98, in this process.

ACKNOWLEDGMENT

The authors wish to thank L. Wayne Schultz for assistance with structural analyses and figure generation, and Dr. Schultz, Jennifer L. McKenzie, Bradley R. Kelemen, and Chiwook Park for helpful discussions and comments on this manuscript. We are grateful to Peter Friedhoff for advice about the synthesis of deoxythymidine 3′,5′-bis-(*p*-nitrophenyl phosphate), and Volker M. Vogt for providing a cDNA encoding I-*Ppo*I. CD data were obtained at the University of Wisconsin—Madison Biophysics Instrumentation Facility, which is supported by the University of Wisconsin-Madison and grant BIR-9512577 (NSF). Finally, we are grateful to Promega Corp. for their generous support of our work on I-*Ppo*I endonuclease.

REFERENCES

1. Perlman, P. S., and Butow, R. A. (1989) *Science 246*, 1106−1109.
2. Mueller, J. E., Bryk, M., Loizos, N., and Belfort, M. (1993) in *Nucleases* (Linn, S. M., Lloyd, R. S., and Roberts, R. J., Eds.) pp 111−143, Cold Spring Harbor Press, Cold Spring Harbor, NY.
3. Argast, G. M., Stephens, K. M., Emond, M. J., and Monnat, R. J., Jr. (1998) *J. Mol. Biol. 280*, 345−353.
4. Wittmayer, P. K., McKenzie, J. L., and Raines, R. T. (1998) *Gene 206*, 11−21.
5. Dujon, B. (1989) *Gene 82*, 91−114.
6. Muscarella, D. M., and Vogt, V. M. (1989) *Cell 56*, 443−454.
7. Dujon, B., Belfort, M., Butow, R. A., Jacq, C., Lemieux, C., Perlman, P. S., and Vogt, V. M. (1989) *Gene 82*, 115−118.
8. Ellison, E. L., and Vogt, V. M. (1993) *Mol. Cell. Biol. 13*, 7531−7539.
9. Wittmayer, P. K., and Raines, R. T. (1996) *Biochemistry 35*, 1076−1083.
10. Muscarella, D. E., Ellison, E. L., Ruoff, B. M., and Vogt, V. M. (1990) *Mol. Cell. Biol. 10*, 3386−3396.
11. Lowery, R., Hung, L., Knoche, K., and Bandziulis, R. (1992) *Promega Notes 38*, 8−12.
12. Ruoff, B., Johansen, S., and Vogt, V. M. (1992) *Nucleic Acids Res. 20*, 5899−5906.
13. Flick, K. E., McHugh, D., Heath, J. D., Stephens, K. M., Monnat, R. J., Jr., and Stoddard, B. L. (1997) *Protein Sci. 6*, 2677−2680.
14. Flick, K. E., Jurica, M. S., Monnat, R. J., Jr., and Stoddard, B. L. (1998) *Nature 394*, 96−101.
15. Tartof, K. D., and Hobbs, C. A. (1987) *Bethesda Res. Lab. Focus 9*, 12.
16. Kunkel, T. A., Roberts, J. D., and Zakour, R. A. (1987) *Methods Enzymol. 154*, 367−382.
17. Nguyen, L., Jensen, D., and Burgess, R. (1993) *Protein Express. Purif. 4*, 425−433.
18. Pace, C. N., Vajdos, F., Fee, L., Grimsley, G., and Gray, T. (1995) *Protein Sci. 4*, 2411−2423.
19. Ferrin, T. E., Huang, C. C., Jarvis, L. E., and Langridge, R. (1988) *J. Mol. Graphics 6*, 13−27.
20. Cuatrecasas, P., Wilchek, M., and Anfinsen, C. B. (1969) *Biochemistry 8*, 2277−2284.

21. Friedhoff, P., Franke, I., Krause, K. L., and Pingoud, A. (1999) *FEBS Lett. 443*, 209−214.
22. Fickling, M. M., Fischer, A., Mann, B. R., Packer, J., and Vaughan, J. (1959) *J. Am. Chem. Soc. 81*, 4226−4230.
23. Thompson, J. E., and Raines, R. T. (1994) *J. Am. Chem. Soc. 116*, 5467−5468.
24. Kolmes, B., Franke, I., Friedhoff, P., and Pingoud, A. (1996) *FEBS Lett. 397*, 343−346.
25. Kraulis, P. J. (1991) *J. Appl. Crystallogr. 24*, 946−950.
26. Johnson, W. C., Jr. (1990) *Proteins: Struct., Funct., Genet. 7*, 205−214.
27. Herschlag, D., and Jencks, W. P. (1987) *J. Am. Chem. Soc. 109*, 4665−4674.
28. Beese, L., and Steitz, T. A. (1991) *EMBO J. 10*, 25−33.
29. Piccirilli, J. A., Vyle, J. S., Caruthers, M. H., and Cech, T. R. (1993) *Nature 361*, 85−88.
30. Eckstein, F. (1985) *Annu. Rev. Biochem. 54*, 367−402.
31. Cleland, W. W., and Hengge, A. C. (1995) *FASEB J. 9*, 1585−1594.
32. Newman, M., Strzelecka, T., Dorner, L. F., Schildkraut, I., and Aggarwal, A. K. (1995) *Science 269*, 656−663.
33. Miller, M. D., Tanner, J., Alpaugh, M., Benedik, M. J., and Krause, K. L. (1994) *Nat. Struct. Biol. 1*, 461−468.
34. Miller, M. D., Cai, J., and Krause, K. L. (1999) *J. Mol. Biol. 288*, 975−987.
35. Friedhoff, P., Kolmes, B., Gimadutdinow, O., Wende, W., Krause, K. L., and Pingoud, A. (1996) *Nucleic Acids Res. 24*, 2632−2639.
36. Friedhoff, P., Franke, I., Meiss, G., Wende, W., Krause, K. L., and Pingoud, A. (1999) *Nat. Struct. Biol. 6*, 112−113.
37. Aggarwal, A. K., and Wah, D. A. (1998) *Curr. Opin. Struct. Biol. 8*, 19−25.
38. He, Z., Crist, M., Yen, H., Duan, X., Quiocho, F. A., and Gimble, F. S. (1998) *J. Biol. Chem. 273*, 4607−4615.
39. Turmel, M., Otis, C., Cote, V., and Lemieux, C. (1997) *Nucleic Acids Res. 25*, 2610−2619.
40. Jurica, M. S., Monnat, R. J., Jr., and Stoddard, B. L. (1998) *Mol. Cell 2*, 469−476.
41. Jeltsch, A., Alves, J., Wolfes, H., Maass, G., and Pingoud, A. (1993) *Proc. Natl. Acad. Sci. U.S.A. 90*, 8499−8503.
42. Horton, N. C., Newberry, K. J., and Perona, J. J. (1998) *Proc. Natl. Acad. Sci. U.S.A. 95*, 13489−13494.

BI991452V